Whole Eye Optical Coherence Tomography (OCT) to Improve Refractive Surgery and Eye Care

Document Date: August 14, 2014

NCT03219567

SIGNIFICANCE

Optical coherence tomography (OCT) is a non-contact, micrometer scale imaging technique which is widely used in clinical eye care and research. In 2010, it was estimated that over 16 million clinical ophthalmic OCT procedures were performed in the United States alone [5]. This averaged one OCT performed on a patient's eye every 2 seconds in the U.S., not even including research OCT usage.

OCT is widely used because in contrast to other clinical imaging techniques, it provides clinicians and researchers with high resolution *in vivo* images sufficient to visualize layered microanatomy. Initially, these images were used qualitatively to describe features and note presence or absence of pathology. Simple quantitative measures such as layer thicknesses of the cornea or the retina were introduced subsequently [6]. More sophisticated quantitative geometric measures such as curvature, slopes, and other volumetric descriptors of shape in the cornea, retina, and optic nerve head have been recently described [7-9]. OCT images, however, are subject to geometric, refractive, and motion artifacts during acquisition [1-4]. This results in spatial distortions in OCT images of the eye, and affects even simple measurements on that representation of the eye (Fig. 1). Though current OCT systems have small fields of view (10°) that limit the effect of some of these distortions for simple measures, quantitative geometric measures will be increasingly impacted by the rapid development and imminent advent of wide-field (40° to nearly 90°) OCT systems both in research and commercially [10-12].

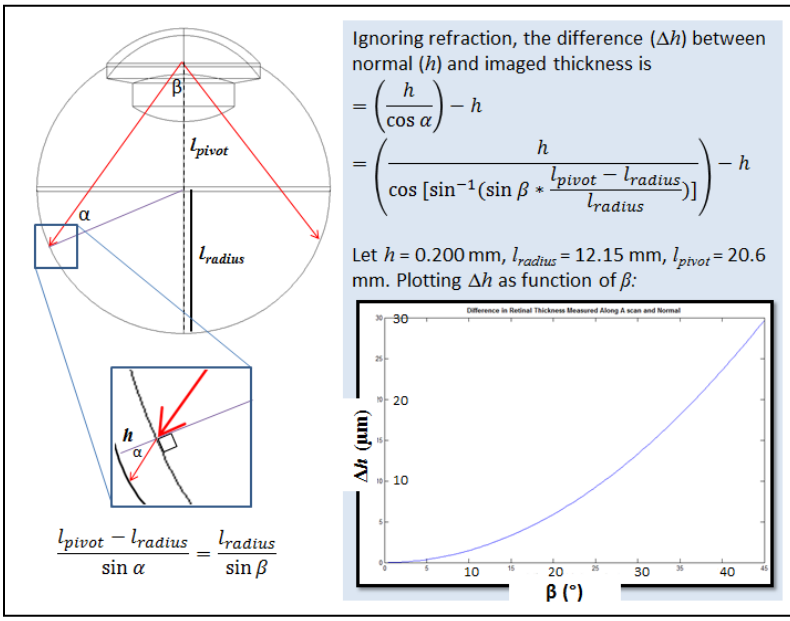

Figure 1. Proof of principle demonstration of differences in peripheral retinal thickness measurements using OCT. The OCT beam is shown in red pivoting through the iris. The eye model is based on published schematic eyes [52,58]. The desired thickness is the surface normal thickness h. The OCT measured thickness is along the A scan in red. The difference between h and the OCT measured thickness increases as the half scan angle β increases.

To faithfully represent the eye using OCT requires a full understanding of the distortions introduced by the entire optical train from the OCT system through the eye's own optics, particularly for retinal imaging [1-3,13-16]. Because of light source and optical limitations, current clinical OCT implementations cannot image the entire eye in a single acquisition (despite a Photoshop-ed "whole eye" OCT in a marketing brochure [12]). A few research groups have begun to address this limitation using multiple reference arms [17] or vertical cavity surface emitting laser (VCSEL) sources with meter-scale fall-off [18] to achieve axial imaging ranges sufficient to image to the back of the eye. Our group was the first to publish the combination of a technology with sufficient axial range for whole eye OCT (coherence revival) combined with dedicated polarization-encoded dual-channel optics designed for optimal imaging of each depth region [19]. Without these dedicated optics, the lateral imaging range and resolution of ocular images from OCT are compromised, regardless of the axial range of the system [18]. Additionally, our group has been among the leaders in developing algorithms to remove refractive and geometric distortions in both anterior and posterior eye images to improve the quantitative accuracy of OCT representations of the eye, particularly for diagnostic measurement of morphology [1,4,20].

In this proposal, we will develop the hardware systems and software algorithms necessary to enable simultaneous OCT imaging of all the refractive surfaces of the eye. We will apply these technical advances to two specific clinical applications where accurately measuring the surface geometry is an important diagnostic task. These clinical aims will also validate the OCT measurement accuracy throughout the eye.

In the front of the eye, enabling accurate measurement of the corneal shape after LASIK and other laser refractive surgeries in over 12 million patients who have had these procedures is a recognized research priority of the National Eye Institute [21]. The inability of current diagnostics to accurately measure the post-surgical corneal shape has resulted in unexpected hyperopia after subsequent cataract surgery [22]. For these patients who were previously accustomed to good spectacle free vision, post-surgical hyperopia means complete dependence on glasses for all distances. A large number of compensatory algorithms have been

offered for this measurement problem, and the net result clinically is that cataract surgery planning for this population is confusing and outcomes are unpredictable [23]. This unpredictability is difficult in a clinical environment where patients routinely expect 20/20 spectacle free vision after refractive and cataract surgeries.

In the back of the eye, measuring surface geometry is also diagnostically important (please see supporting letter from Collaborator Terri Young, M.D.). The standard simple axial length measure has proven inadequate for understanding the myopic (near-sighted) eye and its development. Specific three-dimensional alterations in the shape of the posterior eye in those with myopia have been correlated with progression of this disease [24] and with vision threatening pathology [25,26]; hence, posterior eye shape could be used for risk-stratification with appropriate follow-up and counselling. Recently, off-axis peripheral treatment of refractive error (not standard axial refractive correction) has demonstrated promising arrest of myopia development [27]. Though it would be reasonable to measure posterior eye shape with long available ophthalmic ultrasound, a search of the literature (PubMed using "eye" AND "shape" AND "myopia" AND "ultrasound") returned only one paper using ultrasound for this purpose [28]; the remainder used ultrasound only to measure axial length. Instead, posterior eye shape is currently obtained using MRI [24-26,29-31] with its attendant cost and logistical barriers. Lowering the cost and logistical barriers to obtaining the shape of the posterior eye using ubiquitous, non-contact OCT would allow more widespread clinical use of this measurement for risk stratification of myopes and for study of myopia progression. Further, using OCT provides a 10-fold increase in resolution over posterior segment ophthalmic ultrasound for measurement accuracy and also provides the layered microanatomy that is used widely by clinicians and researchers.

Our contribution will be significant because we will address the important problem of distortions inherent to widely used ophthalmic OCT that impact quantitative measurements from those images, particularly with imminent wide-field implementations.

Our proposed project will improve clinical care by two immediate clinical applications. First, measuring post LASIK corneal power and anterior segment biometry will improve cataract surgery outcomes in this large population, thus reducing potential physical and financial costs associated with unpredictable visual outcomes. Second, by using OCT to recover the shape of the posterior eye, our proposed project makes this diagnostic biomarker widely available clinically and for research. OCT is already used clinically in patients ranging from infancy (without sedation) to adulthood, and would be significantly less costly than MRI for this purpose.

Achieving our aims will change ophthalmic diagnostic imaging by enabling widely used OCT to produce accurate, faithful representations of the imaged eye as a whole with broader implications for improving the accuracy and reliability of any quantitative measurements based on OCT images.

INNOVATION

The proposed research is innovative because it challenges the conventional representation of the eye in OCT images by recognizing the eye as a complete optical system, and not as non-interactive anterior and posterior regions. By considering the image forming contributions of the whole eye, our OCT hardware and software developments will produce quantitatively accurate representations of both the anterior and posterior eye. The expected innovations include:

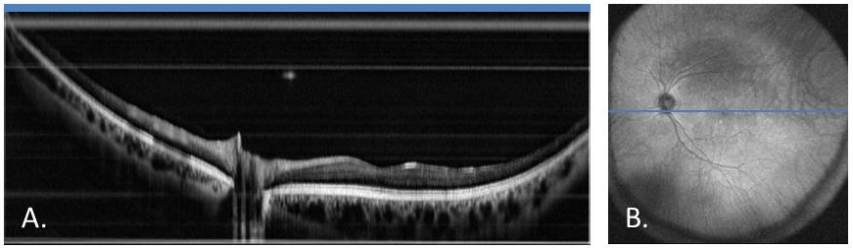

FIGURE 2. Ultra-wide field swept-source retinal OCT at 1060nm. Results from prototype system imaging with 85° FOV on the retina relative to the posterior nodal point of the eye. Representative B-scan (A) and summed voxel projection (B) are shown. Layered retinal structures are visualized over the complete field of view.

1. Novel optomechanical hardware designs to enable simultaneous imaging of both the front and back of the eye with focused fields of view <u>larger</u> than current systems dedicated to only the front or the back of the eye (Fig. 2).
2. Hardware and algorithm/software developments to remove the effects of motion and optical artifacts that corrupt the accuracy of anterior eye OCT. This will enable three-dimensional anterior segment biometry with OCT for clinical use in surgically and non-surgically affected corneas.
3. In addition to the above, algorithmic developments to remove the effects of optical artifacts that distort the spatial accuracy of posterior eye OCT. This will enable three-dimensional posterior segment biometry with OCT for clinical and research use in myopia and other posterior eye applications.

Together, these innovations will produce a spatially accurate portrayal of the eye from ophthalmic OCT and provide a solid foundation for all quantitative measurements on the imaged eye. Our previous studies which have laid the groundwork for all of these innovations [19,32,4] strongly suggest that these advances will improve the diagnostic accuracy of OCT derived measurements for both the front and back of the eye. This departure from the status quo is expected to enable the widely available OCT platform to faithfully represent the imaged eye.

APPROACH

Specific Aim 1: Develop hardware modifications to OCT to allow simultaneous imaging of both the anterior and posterior eye.

SA1. Introduction. To produce images of the eye accurate enough to perform surface metrology, we require images containing all of the important optically refracting surfaces in both the anterior (cornea, lens) and posterior eye (retina). By directly imaging both the anterior and posterior eye, optical analyses of the eye can then be performed directly on the imaged optical surfaces. To produce a sharply focused OCT image at both the anterior and posterior eye requires deliberate design because the imaging paths to these two locations are optically different.

The *objective* of this aim is to develop the optomechanical modifications to the usual OCT topology that will enable, at minimum, focused standard field of view (FOV) images of both the anterior and posterior eye simultaneously. Simultaneous capture ensures co-registration of the anterior and posterior images to produce single, unified representations of the eye.

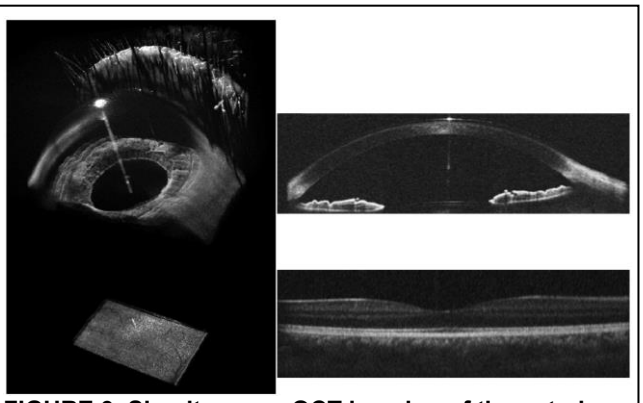

FIGURE 3. Simultaneous OCT imaging of the anterior and posterior eye from our previous work [19]. Both volumetric renderings (left) and representative constitutive B-scans (right) are shown. Of note, the FOV and resolution of the simultaneously acquired images are both comparable to images acquired from dedicated anterior or posterior eye OCT systems. (The anterior and posterior eye images do not share the same scale.)

The *rationale* for this aim is that successful completion of this aim will produce OCT images of the major ocular surfaces that are optically accessible. Our *expectation* is that the image volumes produced by this system will contain the information necessary to improve the accuracy of the represented eye for subsequent optical analysis, image distortion correction, and diagnostic use.

SA1. Justification & Feasibility. While there have been prior implementations of simultaneous whole eye OCT systems [14,15], those implementations were intended primarily to measure distances to various surfaces. These systems utilized telecentric scanning focused on the anterior eye. Posterior eye images from these systems had extremely limited FOV due to telecentric scanning at the anterior eye; in fact, when refraction corrected, the retinal FOV from these systems was an oversampled small spot. These systems also lacked lateral resolution at the macula because the system focus was designed for the anterior eye. While these limitations do not hamper measurement of distances, dedicated wider fields of view focused on the retina are required to truly study the posterior eye.

Our team has developed the component technologies for an OCT system that is capable of simultaneous, focused imaging of both the anterior and posterior eye [19]. In this system, the OCT light is divided using polarization into anterior and posterior eye channels. Both paths independently image their respective area of the eye simultaneously. On return, the coherence revival technique unique to specific swept source lasers is used to encode the different imaged depths [33]. This provides both correction of the complex conjugate artifact for extended imaging range in the anterior eye, as well as depth multiplexing with separation of the anterior and posterior eye scans within the final images. An image volume of a living subject's eye obtained with this system after post-processing is seen in Figure 3.

While this system demonstrated the feasibility of simultaneous dual depth imaging with OCT using only a single source and detector, this demonstration system will require additional design to achieve the goals of this proposal. Most notably, the anterior eye channel of this system was not designed to image the anterior eye from the cornea to the lens, and the posterior eye FOV was less than the usual 30° in standard ophthalmic photography. With this demonstration system as a basis, however, we will make informed design modifications to improve this system for the stated aims of this proposal.

SA1. Research Design. *Whole eye OCT system design.* The basic OCT configuration consists of the source, detector, sample arm, and reference arm. To meet the clinical needs of this project, we will substantially

redesign the sample arm (Fig. 4). There will be three major changes: 1. Redesign of the anterior eye channel optics to enable imaging from the anterior cornea to the posterior lens, 2. Redesign of the posterior eye channel optics to increase the FOV, and 3. Redesign of the galvanometer pair configuration to ensure uniform, symmetric scanning. An iris camera will also be added to aid clinical use and alignment.

The anterior eye channel requires redesign to enable imaging from the anterior cornea to the posterior lens. Nominal values for the component thicknesses in a 60 year old are as follows: cornea thickness 0.5 mm, anterior chamber depth 2.86 mm, and lens thickness 4.24 mm [34]. Together this suggests that an imaging depth on the order of 7.6 mm is required for full anterior eye imaging. For OCT, there are both signal (falloff) and optical considerations that affect imaging depth range. From a signal standpoint, the 6 dB falloff range for our prior coherence revival SS-OCT system was 8.5 mm [19]; this exceeds our nominal requirement. We also expect a slight increase in this range with increased digitizer bandwidth in the newer planned system.

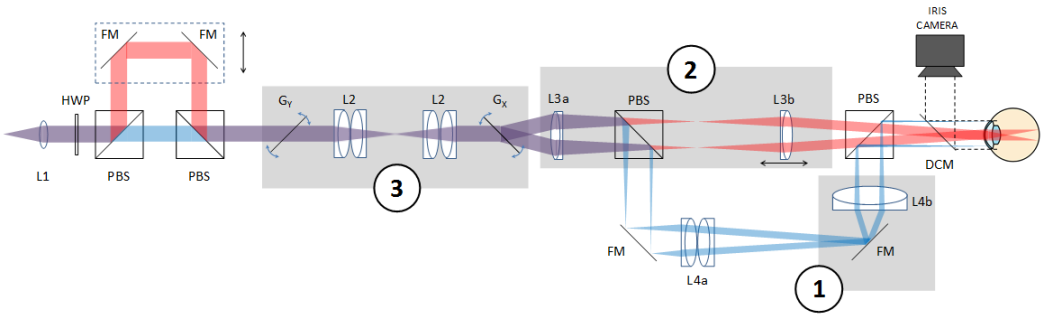

FIGURE 4. General schematic of sample arm design for simultaneous OCT imaging of the anterior and posterior eye (similar to our previous design in [19]). This design relies on polarization encoding to separate the light source (purple) into anterior (blue) and posterior (red) eye paths. Dedicated optics for the anterior and posterior eye paths allow for optimal imaging of each location even through acquisition is occurring simultaneously. In the first specific aim, we will redesign: (1) anterior eye optics for increased depth of focus, (2) posterior eye optics for increased FOV, and (3) galvanometer pair to include a 4F, 1x relay. L1: collimating lens, HWP: half wave plate, FM: fold mirror, PBS: polarizing beam splitter, G_Y/G_X: 1D galvanometers, L2: 4F telescope with1X magnification to image G_Y onto G_X, L3a-b: retinal telescope (L3b is adjustable to optimize focus at the posterior eye), L4a-b: anterior eye optics, DCM: dichroic mirror for iris camera.

Optically, we need to increase our depth of focus (DOF) to image through the desired depth range. Increasing DOF, however, will decrease the lateral resolution. To determine the appropriate balance between DOF and lateral resolution, we consider our requirements. Commercial anterior eye OCT systems with sources 1000 nm or greater have reported resolutions of 10-18 μm axially and 30-60 μm laterally. Using the minimum of these parameters as guidance, we have created an initial anterior eye sample arm design with a DOF of 6.7 mm and a theoretical full width-half max lateral spot size of 39.5 μm in air. Coupled to our 1060 nm SS-OCT engine with a measured axial resolution of 7.8 μm in air, we were able to produce an image of the entire anterior eye with this preliminary sample arm design (Fig. 5).

Regarding the posterior eye channel, redesign is required to increase the FOV to measure posterior eye shape. Figure 2 shows the imaging results from a preliminary posterior eye sample arm built with large diameter double aspheric optics which produces 85° FOV. This is nearly triple that of standard ophthalmic photography, and all major posterior ocular features (optic nerve, macula, vascular arcades) are visible while still retaining high axial resolution as evidenced by presence of layered microanatomy in the B-scan. Also the system is implemented at 1060nm, enabling penetration through the full choroidal depth.

Together, the re-designed anterior and posterior eye imaging sub-systems meeting our design requirements shown in Figs. 2 and 5 will be incorporated into the polarization-encoded, coherence-revival based system depicted in Fig. 4 to accomplish true whole eye OCT – simultaneous anterior and posterior eye OCT with optimal focusing and large fields of view at both locations – for the first time.

The light source for this whole eye OCT will be the same commercial external-cavity tunable swept source laser operating with a nominal center wavelength of 1060 nm, 100 nm tuning bandwidth, and sweep rate of 100 kHz (Axsun Technologies) used in our previous work. A balanced receiver detection design will be used with a 1 GHz InGaAs balanced receiver (WL-BPD1GA, Wieserlabs) and digitized at 1.8 GS/s on a 12 bit (9.1-ENOB) digitizer (ATS9560, Alazar Tech). This digitizer has larger bandwidth (800 MHz) than the original system (500 MHz) which will decrease fall off and increase SNR farther from DC. Otherwise, the detection design reflects what was used in our earlier system to achieve dual depth, coherence revival imaging.

The complete system will be assembled into a rack mountable breadboard and case to allow use in the clinical environment without exposed optical elements. The sample arm will be mounted onto an adjustable, portable table with head rest and chin rest for patient comfort and to minimize gross patient movement. The reference mirror will be on a ruled translation stage to allow calibration of system to eye distance as described

below. The system will be controlled by custom software written in C++ utilizing GPU coding for real time OCT data processing and display at 100 kHz A-scan rate.

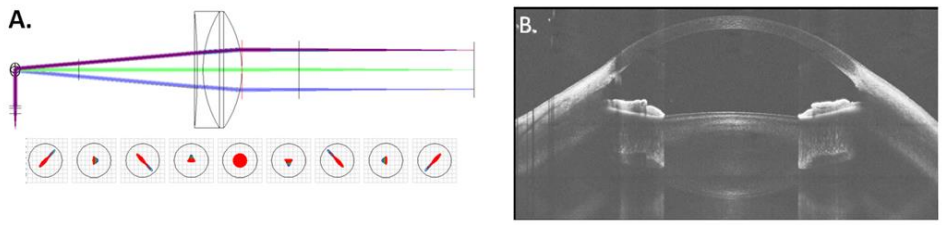

FIGURE 5. (A) Increased depth range anterior eye sample arm and (B) resultant image quality in a human subject. This sample arm design has fields of view of 17 x 17 mm, depth of focus of 6.7 mm, and a theoretical lateral full width-half max spot size of 39.5 µm. The resultant image shows both the anterior and posterior cornea and the anterior and posterior lens. Vertical artifacts from increased light reflection at the iris and sclera are present in this iteration of the system design. Within the pupillary zone ("optical zone" of the eye), these brighter artifacts are not present. The OCT engine is the same as used in our prior work [19].

System calibration for quantitative analysis. Once the system is assembled, the sample space of this system will need to be characterized for subsequent quantitative analyses as we have done in past work [20]. There are three primary quantities which will need to be calibrated: distance of system to the sample (eye), lateral pixel pitch, and axial pixel pitch. The lateral and axial pixel pitches define the sample space dimensions within the digital image and is determined by imaging a dual-axis linear-scale stage micrometer (NT58-763; Edmund Optics).

The system to eye distance affects magnification and telecentricity of the scan and can be determined from the zero path length delay (ZPD) in the anterior eye image. The location of the ZPD in the image is equivalent to the reference mirror position in Fourier domain OCT. To calibrate the system, we will image a flat target in air at a known, measured distance (close to the working distance) from the final optic of the sample arm. We will then adjust the reference mirror until the image of that flat target is at the ZPD within the anterior eye channel image. At this calibrated reference position, ZPD in the image represents a known distance from the final sample arm optic within the image. During clinical imaging, the distance from the final sample arm optic to the cornea (eye) will be measured by adding the known distance to the ZPD (calibrated) to the distance between ZPD and the corneal apex in the image. Any reference arm translation from the initially calibrated position is simply measured from the translation stage and added to the ZPD to cornea distance to determine the final system to eye distance. In summary, ZPD in image (ZPD_{image}) = known calibrated distance from final optic of system, ZPD to cornea (cornea-ZPD) = measured from image, reference arm translation from initial calibrated position (Δref) = measured from translation stage. The final system to eye distance = ZPD_{image} + (cornea-ZPD) + Δref. Distances to the posterior eye image content will be determined by measuring the fixed one laser cavity length offset from the anterior eye image used for coherence revival [19,32]. With system to eye distances known, we will accurately account for magnification and non-telecentricity optical artifacts affecting the imaged ocular structures.

SA1. Expected Outcomes. This aim will produce an OCT system capable of simultaneous clinical imaging of the anterior and posterior eye. For the anterior eye channel, the resolution will be sufficient to measure corneal power and the imaging range sufficient to image from the front of the cornea to the posterior lens. For the posterior eye channel, the FOV will nearly triple standard ophthalmic photography (85° FOV relative to nodal point) with resolutions comparable to current retina-only OCT systems. As a whole eye system, both channels will be imaging simultaneously to produce coregistered volumes of all meaningful surfaces of the eye. The sample space of this system will also be characterized sufficiently to perform clinical surface metrology on the images of the eye. With this information, accurate clinical measurements for anterior segment biometry and posterior eye shape recovery can be performed.

SA1. Potential Problems & Alternative Strategies. While we are confident that the coherence revival imaging strategy proposed above is readily extendable for whole eye imaging, it is possible that by the time this proposal is funded, alternative technologies to coherence revival such as a 1050 nm VCSEL source may become commercially available which would simplify the required technology development. If so, we will take full advantage of this by incorporating this source with our dual depth sample arm optics to obtain full fields of view for the posterior segment; otherwise, the VCSEL source alone only scans a small spot posteriorly [18].

Finally, we also recognize that there are ambiguities inherent to image reconstruction in the presence of the phakic (natural) lens. This is specifically addressed in the posterior eye reconstruction aim (SA3.Research Design and SA3.Potential Problems). In short, we will take a systematic approach starting with imaging of pseudophakic subjects (artificial lens of known optical prescription) for validation of the reconstruction algorithms followed by imaging of phakic subjects with reconstructions utilizing published gradient index models of the natural lens.

<u>Specific Aim 2:</u> Develop and validate algorithms to produce accurate three-dimensional anterior eye OCT reconstructions for use in post LASIK cataract surgery patients.

SA2. Introduction. Clinically measuring the refractive power of the post-LASIK cornea has proven to be a challenge with current diagnostics; this has led to unpredictable cataract surgery outcomes for these individuals who previously enjoyed high quality spectacle free vision after LASIK. The post-LASIK cornea violates assumptions made by current diagnostics to determine whole corneal power from a single measurement of the anterior corneal surface. While corneal power is thought to be the predominant factor in this problem, modern cataract surgery also requires other anterior segment biometric measures in its determination of intraocular lens power. These anterior segment biometric measures include anterior chamber depth and corneal diameter and are used in conjunction with corneal power (curvature) to determine the estimated lens position (ELP).

Tomographic techniques such as OCT image the cornea in whole (anterior surface, posterior surface, and intervening stroma), and hence OCT requires fewer assumptions than current diagnostics for measuring corneal power [35]. However, to utilize anterior eye OCT images for measuring the corneal refractive power, the acquired OCT images need to be faithful representations of the imaged eye. As a scanned light technique, OCT light is affected by transit through the imaging system, by transit through the imaged eye, and by motion of the imaged eye during scanning. These corrupting artifacts need to be addressed and removed from the images to create faithful representations of the anterior eye. Once the images are corrected, algorithms to recover the pertinent clinical values from the imaged structure can be used.

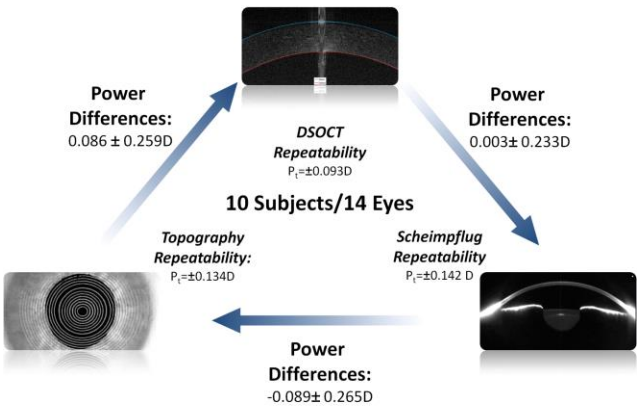

FIGURE 6. Comparison of corneal refractive power measurements between motion corrected distributed scanning OCT (DSOCT), *top*, and the clinical standards (topography, *bottom left* and Scheimpflug photography, *bottom right*) [32]. In these normal corneas, the mean difference between OCT and the two clinical standards is less than 0.10 D with a standard deviation approaching the clinical refraction resolution of 0.25 D.

Time-domain OCT (Zeiss Visante) was one of the first OCT devices used for the purpose of anterior segment biometry [36]. However, motion artifacts due to its slow acquisition rate reduced the reliability of its measurements [7]. With the substantial speed and resolution increase from spectral-domain OCT, accurate spherical corneal power measurements have been shown [34,36]. Compared to clinical standards, though, the P.I. has shown that the standard deviation of SDOCT measures was higher than clinical resolution [37]. With dedicated motion correction techniques, this variability decreased to clinical resolution [32], suggesting the speed of conventional SDOCT alone was not sufficient to mitigate motion artifacts. With motion correction, we were also able to measure true OCT based corneal topography [38]. This global corneal surface measurement has not been available with clinically available OCT systems likely due in part to motion artifacts. Also, in contrast to the slower Visante, the limited depth range of SDOCT does not allow the measurement of anterior segment biometry as used in OCT based intraocular lens selection [36].

The objective of this aim is two-fold. The *first objective* is to develop and validate algorithms for the accurate measurement of anterior segment biometry from OCT images including clinical corneal spherical and astigmatic powers and anterior segment dimensions (such as anterior chamber depth and width). The *second objective* is to test the hypothesis that improved anterior segment biometry measurement with OCT will improve cataract surgery outcomes in patients with prior LASIK.

The *rationale* for this aim is that successful completion of this aim will produce OCT images of the anterior eye faithful enough for accurate anterior segment biometry. In addition to the clinical rationale, this aim also serves to validate anterior segment measures for the posterior segment aim. Our *expectation* is that the more accurate measurement of anterior segment biometry will remove uncertainty in optical characterization of the post-LASIK eye and improve cataract surgery outcomes in this population.

SA2. Justification & Feasibility. Utilizing current commercially available spectral domain OCT (SDOCT) systems, the PI has led development and implementation of a suite of technologies that address automated segmentation, motion and optical artifact removal, and measurement of pertinent clinical parameters from OCT images of the cornea [20,32,37,39]. In these works, we have shown that we can accurately measure surface curvatures of manufactured phantoms with less than 10 μm difference from the nominal manufacturer values

and with better than 10 μm repeatability. In clinical work, we have shown in normal, non-surgically altered corneas that we can measure the corneal refractive power with SDOCT comparable to existing clinical standards (Fig. 6). The mean difference of the SDOCT measured corneal power against the clinical standards was less than 0.10 D. The standard deviation with motion correction was only 0.25 D (14 eyes). Repeatability of measurements was under 0.12 D. For clinical context, glasses prescriptions are measured at intervals of 0.25 D.

We have performed a preliminary clinical study demonstrating the ability of SDOCT to measure the corneal power change due to LASIK [40]. In LASIK, the excimer laser reshapes the anterior cornea to change the eye's refraction. Hence, the measured refractive change in an eye before and after LASIK should ideally equate to the change in measured corneal curvature and power. To test this, 39 eyes of 22 patients were enrolled in a Duke University Institutional Review Board (IRB) approved study before they underwent LASIK. The enrolled subjects underwent preoperative imaging with topography, Scheimpflug photography, and SDOCT and received a manifest refraction (MRx) prior to LASIK. The same measurements were then performed at least 3 months after LASIK when visual acuity stabilized. Table 1 summarizes the results.

	MRx – Topography	**MRx – Scheimpflug**	**MRx – OCT**
$\Delta\Phi_K$ (D)	-0.50 ± 0.68 p = <0.001 *ICC* = 0.92 (0.85-0.96)	0.06 ± 0.85 p = 0.714 *ICC* = 0.94 (0.88-0.97)	0.13 ± 0.60 p = 0.216 *ICC* = 0.96 (0.93-0.98)
$\lvert\Delta\Phi_K\rvert$ (D)	0.72 ± 0.45	0.53 ± 0.66	0.48 ± 0.37

Table 1. Imaged corneal power change from LASIK compared to vertexed manifest refraction (MRx) change

In this LASIK population, the mean absolute difference (colored row in Table 1) is the pertinent metric as it represents any deviation, positive or negative, from the reference MRx measure. As a point of reference, the step size of intraocular lenses is 0.50 D. Topography was found to be significantly different from the reference manifest technique ($p < 0.001$, t-test with generalized estimating equations). On average, the SDOCT measurement deviated least from the refractive change and was the least variable. The variability of the Pentacam (Scheimpflug) measurement is unacceptably high; as a result of other studies (not this one), Pentacam is no longer on the American Society of Cataract and Refractive Surgeons' clinically accepted modality list (iol.ascrs.org).

In addition to spherical measures, we were also able to use OCT to characterize changes in astigmatism as seen in Figure 7. In our population, the mean paired difference between the surgically induced change in manifest astigmatism and OCT was 0.49 D ± 0.37 D. This was lower than that found with topography simulated keratometry (0.60 D ± 0.51 D) which was found to be significantly different from the reference manifest technique ($p = 0.003$, t-test with generalized estimating equations).

Overall, these preliminary results show that our OCT based corneal reconstructions are sufficiently accurate to measure the corneal power change both spherically and astigmatically resulting from LASIK.

SA2. Research Design. *Algorithm development and validation.* In contrast to the SDOCT system that we used for our preliminary data above, the proposed whole eye SSOCT system will provide deeper and wider anterior eye views, while simultaneously imaging the posterior eye. There are multiple benefits to this. First, imaging more of the anterior eye will allow for complete anterior segment biometry measurements which can be used to improve intraocular lens selection [41-45]; the cornea alone is not the only determinant of intraocular lens power. Secondly, the co-registered posterior eye image from whole eye OCT will also allow for definition of the visual axis to provide a functional reference axis for the corneal power measurement.

With the raw anterior eye OCT images, the following post-processing algorithms will be applied: segmentation of ocular surfaces, removal of optical and motion artifacts, and finally recovery of the desired clinical parameters. For segmentation, we will use our prior dynamic programming based algorithms [39] and modify them to account for the wider FOV in the whole eye OCT system. In addition, these intensity and graph based algorithms will be extended to segment the iris surface to identify the pupil location.

For removal of optical artifacts, we will directly apply our prior, validated three-dimensional refraction correction algorithms [20]. Successful 3D refraction correction requires accurate characterization of sample arm scanning geometry, sample space, and refractive indices. The scanning geometry is known from our Zemax design, and sample space will be calibrated as described in Aim 1 and [20]. Refractive indices for OCT based refraction correction requires knowledge of the group (not phase) refractive index at the wavelength of interest. Co-Investigator Dr. Izatt, in collaboration with OCT inventor Dr. David Huang, first described physical measurement of the group refractive index of samples (such as the cornea) using OCT in 2004 [46]. Briefly, a cuvette of known, calibrated internal chamber thickness is imaged and measured first. Then a representative sample (for example, calibration phantom or fresh *ex vivo* cornea) is placed in the chamber and the thickness is re-measured. The image provides the resultant optical pathlength change of the chamber as a result of the

sample for that OCT light. Because the empty physical thickness of the chamber has been measured, all quantities necessary to determine the group refractive index for the intervening representative sample at that OCT light bandwidth are known. We have used and validated this technique in our prior work with λ_0 = 840 nm [20,37]. We will do the same for the cornea using averaged *ex vivo* samples with the 1060 nm swept source light used in this project.

For motion correction, our prior distributed scanning OCT technique used both increased acquisition speed and motion estimation to improve measurement of corneal power over standard linear scanning SDOCT [32]. Our distributed scanning acquired an individual corneal profile in 1/5th the time required for a standard linear scan, and after motion estimation, still produced a B-scan of comparable A-scan density to a normal linear scan. The whole eye OCT system operates at an A-scan rate of at least 100 kHz compared to 20 kHz for SDOCT. By applying distributed scanning OCT to our whole eye OCT system, we can achieve another 5-fold decrease in profile acquisition time which should further mitigate any potential motion artifacts. Additionally, the presence of the iris in the whole eye OCT images offers additional image registration targets that can be used for improved motion estimation if needed.

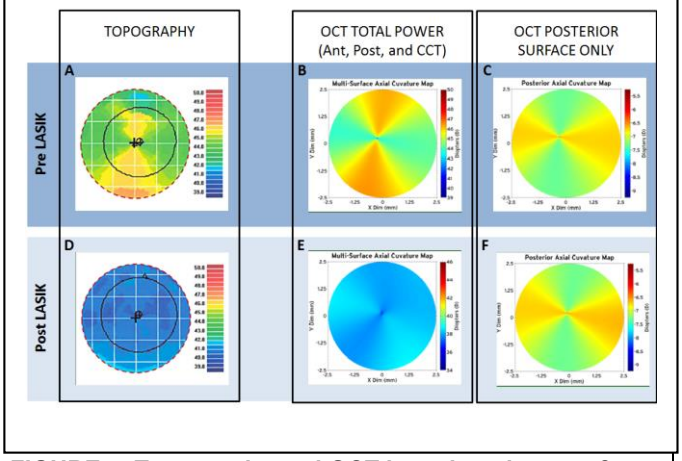

FIGURE 7. Topography and OCT based total power & topography maps. This figure shows that our recovered OCT based surfaces are sufficiently accurate to represent astigmatic information even in corneas altered by LASIK. Before LASIK (top row), topography and OCT are comparable (A & B). After LASIK (bottom row), topography (D) shows an effectively spherical cornea because it is only measuring the ablated anterior surface. In the OCT map (E), residual corneal astigmatism is still present (lighter blue) likely due to the unchanged astigmatic posterior surface (C & F). The measured spherical change pre to post LASIK was: ΔMRx = 5.25 D, Δtopo = 3.94 D, ΔOCT = 5.63 D. The surgically induced change in astigmatism was: ΔMRx = 2.80 D, Δtopo = 2.04 D, ΔOCT = 2.63 D. These maps show the central 5 mm of the cornea.

Finally, the corneal curvatures and refractive powers (both spherical and astigmatic) will be recovered using our previously described algorithms [37,38]. Importantly, we will be able to align our measurements to the reference axis from the entrance pupil to the fovea due to the addition of the iris and posterior eye information from whole eye OCT. This provides an advantage over standard keratometry or standalone corneal OCT which are aligned along an arbitrary and non-functional axis.

We will confirm the accuracy of these anterior eye algorithms for segmentation, artifact removal, and motion correction combined with the whole eye OCT system by using calibration phantoms (glass spheres and contact lenses of known curvature and refractive power) and in an initial small series of 20 normal subjects.

Clinical study. We will enroll subjects who have had previous laser refractive surgery (LASIK, PRK) and who will be undergoing cataract surgery to test the hypothesis that improved corneal power measurement using OCT will improve the refractive outcomes compared to standard of care (Fig. 8). Each enrolled subject must be able to have optical biometry measurements (IOLMaster, Carl Zeiss Meditec) needed for standard of care IOL selection. The optical biometric measurements include corneal power (K), anterior chamber depth (ACD), and axial length (AL) among others. These subjects will also be imaged with the whole eye OCT system. We will then choose two intraocular lens powers predicted to achieve a near emmetropic (plano) outcome:

1. Standard of care (SoC) based on the Haigis-L output recommendation at http://iol.ascrs.org. This IOL calculator website for post refractive surgery eyes is maintained by the American Society of Cataract and Refractive Surgeons (ASCRS) and is readily available to the clinical community. The website has multiple formulas but only two – the Haigis-L and the Shammas-PL – do not require prior records. This is most comparable to an OCT based method which also would not require prior records. We are choosing the Haigis-L because there are prior results in the literature from a small pilot study directly comparing the Haigis-L to a different corneal SDOCT based method [45] which can be used to power our study.

2. Whole eye OCT based. We will use the OCT based vergence tracing formula described in [36]. Current clinical IOL formulas have many assumptions inherent in them such as a non-surgically altered cornea and that estimated lens position is a function of the non-surgically altered cornea [47]. To remove these assumptions which are violated in post LASIK patients, we will recover the pertinent biometry measures directly from whole eye OCT and use the described vergence tracing formula to determine the whole eye OCT recommended IOL. This formula was developed specifically for OCT, but available time domain OCT at that

time was unreliable due to motion artifacts from slow acquisition [36]. Current clinical SDOCT is faster, but its limited depth range prevents measurement of the pertinent biometry values used in this formula. Our whole eye system is faster than SDOCT and has the depth range necessary to measure all the pertinent biometry values required to take advantage of this formula.

After undergoing cataract surgery with an intra-capsular posterior chamber IOL of the surgeon's choice, we will measure the manifest refraction at the final, post-operative month 1 visit. From this post-operative manifest refraction, the IOL power required to have achieved an emmetropic (plano) result will be calculated [45]. We will then compare this calculated reference power to the predicted power from the SoC and OCT methods and determine a prediction error for each. Given that IOLs are only powered in discrete increments of 0.50 D, a "good" clinical outcome should be within 0.50 D of the target. Hence, we will compare the proportion of subjects in the two groups (SoC and OCT) who have prediction errors within ± 0.50 D of the calculated reference. Though finer discrimination than 0.50 D would be desirable, we are limited by the resolution of the IOL at ± 0.50 D steps. We cannot insert a lens that is 20.13 D, for example, if that is the theoretical suggested power. Reporting results within ± 0.50 D is also a standard accepted and used by the refractive surgical community [48].

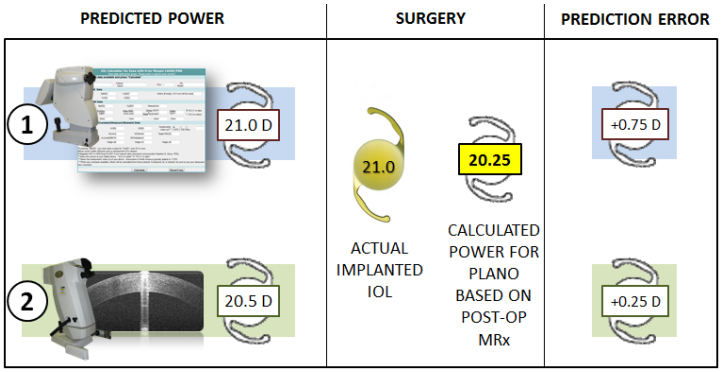

FIGURE 8. Overview of primary clinical outcome to determine if more accurate anterior segment biometry measurement from OCT improves post-LASIK cataract surgery refractive outcomes. Before cataract surgery (left column), we will calculate the needed intraocular lens (IOL) power via (1) standard of care (SoC: 21.0 D in this example) and via (2) our OCT based corneal power and anterior segment biometry measurement (20.5 D). The surgeon will perform cataract surgery and implant an IOL (21.0 D IOL). Based on the post-operative refraction, the power actually needed for a plano result will be calculated (20.25 D). The difference between this calculated reference and the predicted power is the prediction error. We will compare the proportion of SoC and OCT results with prediction errors ≤ 0.50 D.

From the literature, we can estimate the expected proportions for the SoC (P_{SoC}) and OCT (P_{OCT}) groups. Using the Haigis-L, the proportion of subjects who had a result within ± 0.50 D of the calculated reference was approximately P_{SoC} = 41.98% [45,49]. In a small pilot using averaged 2D corneal SDOCT measurements with less sampling than our 3D reconstructions, Tang et al. found the proportion of subjects with a result within ± 0.50 D of the calculated reference to be P_{OCT} = 68.75%. Our null hypothesis is OCT will equal SoC (H_0: $P_{SoC} - P_{OCT} = 0$), and the alternate hypothesis is that OCT will be different (H_A: $P_{SoC} - P_{OCT} \neq 0$). Proportions will be compared using a conditional McNemar's test for paired proportions. Using the estimated proportions, $\alpha = 0.05$, and assuming zero correlation between pairs, we will need a minimum of 60 subjects to complete the study to have 80% power to detect a significant difference between these two proportions (PROC POWER, SAS v.9.3). If the correlation between pairs is 0.2, 60 subjects will provide 88% power; if the correlation is as high as 0.4, the power will be 96%. To account for possible enrollment losses from intra-surgical complications or follow-up losses, we will target an enrollment of 65 subjects over the project period to ensure that we will meet the minimum of 60 completed study subjects.

In addition to the primary outcome measure above, we will additionally report the mean absolute prediction error for the two groups. We will also repeat the optical biometry and OCT imaging post-operatively to further study the relationship between pre-operative biometry and the final IOL position (ELP). These measurements will allow us to further characterize the relationship between clinical optical biometry and the whole eye OCT pre- and post-operatively.

SA2. Expected Outcomes. We will have developed algorithms to accurately measure anterior segment biometry and corneal power with the whole eye OCT system. We will further have clinical data to support the idea that accurate measurement of anterior segment biometry will improve cataract surgery refractive outcomes in those who have previously had laser refractive surgery. While this growing population would particularly benefit because of the unique challenges presented by their altered corneas, the developed algorithms can also be applied for the larger group of cataract surgeries in those with normal corneas as well. Finally this aim also complements the posterior segment aim by independently validating the measurements of anterior segment surfaces by the whole eye OCT system.

SA2. Potential Problems & Alternative Strategies. While we expect that improved anterior segment biometry measurement with OCT will improve cataract surgery outcomes in those with prior LASIK, additional parameters could potentially further reduce the IOL prediction error. For instance, as described earlier, modern

IOL power formulas estimate the final position of the IOL by using the corneal curvature. Interestingly, in recently presented preliminary data [50], a formula which did not utilize corneal curvature for estimating the lens position [51] appeared to do better than those that did use corneal curvature in post LASIK patients undergoing cataract surgery. In our study, we will be obtaining additional biometric measurements pre and post-op – both standard of care and OCT based – to be able to analyze other contributions to the IOL error if there is a systemic bias even after corneal power correction. Regression to these collected data and measurements could be utilized as an alternative approach [45].

Alternatively, other commercially available spectral domain OCT could be used for this aim. However, they currently lack the imaging range necessary to perform the anterior segment biometry required for this aim, and they generally cannot provide a reference axis to the fovea for their corneal measurements. Conversely, the corneal power specific portions of our algorithms could be applied to existing OCT to improve their corneal power measurements and benefit the clinical OCT community in general.

Specific Aim 3: Develop and validate algorithms to produce accurate three-dimensional posterior eye OCT reconstructions to supplant MRI for measuring posterior eye shape in myopia applications.

SA3. Introduction. Current clinical OCT images of the posterior eye are spatially inaccurate. This can be observed simply by noting that almost all clinical OCT images of the retina appear artificially flattened when the expectation is that the eye globe should be curved (Fig. 9). Because of this spatial inaccuracy, OCT cannot in its current form replace MRI for the quantitative study of ocular shape deviations in diseases such as myopia, even though OCT is more clinically accessible and has higher spatial resolution than MRI. Further, the spatial inaccuracy with OCT is compounded by variable optical artifacts from the system and eye, meaning that image differences between patients or time points may not be solely due to pathology as is usually assumed.

The spatial inaccuracy of current posterior eye OCT images results from the current standard practice of simply displaying A-scans next to each other in a parallel fashion. This fails to account for the actual, non-parallel transit of OCT light through the eye. The objective of this aim is two-fold. The *first objective* is to develop and validate algorithms for accurately portraying the posterior eye in OCT images by ray tracing the OCT imaging paths through the imaged anterior eye. The *second objective* is to then test the hypothesis that corrected posterior eye OCT images will be comparable to MRI of the same eyes.

The *rationale* for this aim is that successful completion of this aim will produce posterior eye OCT images faithful enough to replace MRI imaging for studying posterior eye shape biomarkers. Our expectation is that this development will remove cost and logistical barriers limiting more widespread study of posterior eye shape as a diagnostic biomarker for myopia progression, particularly in children and young adults.

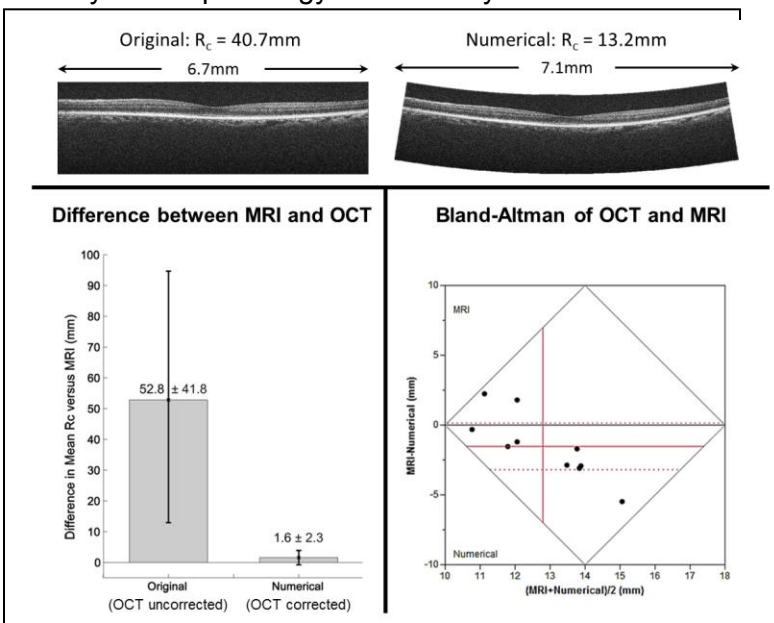

FIGURE 9. Representative original and spatially (numerically) corrected retinal OCT B scans (top R) and comparison to MRI (bottom L and R) [4]. The posterior eye appears flat in the original image (top L) and has a more plausible physiologic curvature after spatial correction (top R). Reported values in the literature for posterior eye curvature (Rc) range from 10.8-14.1 mm [34]. Spatial correction in the 10 eyes in this study significantly reduced the difference between OCT and MRI posterior eye shape (bottom L). In this small preliminary study, there remains a bias and a possible trend between the OCT measures and MRI (bottom R).

SA3. Justification & Feasibility. In an initial study by the P.I. [4], we enrolled subjects in an IRB approved study who had recently obtained head MRIs for their medical care but did not have ocular disease. We performed ocular biometry and retinal SDOCT on these subjects. Using commercial ray tracing software, we modeled the commercial SDOCT system and the subjects' eyes using their measured biometric data. The spatial orientation of the OCT scan paths was then used to reorient each OCT A-scan to its modeled location in MATLAB. Using this correction, there was a significant reduction in differences and variability between posterior eye shape measured by OCT and MRI (Fig. 9).

Despite the overall improvement in posterior eye OCT shape in this pilot study, there remained a bias between the OCT measures and MRI. The possible sources of error in this preliminary work (other than small

sample size) include the lower resolution of these non-orbital MRI scans, the use of schematic model anterior eyes, motion errors, and the unknown system-to-cornea distance to control for scan magnification.

In this proposal, we will perform a prospective study with dedicated orbital MRIs, with measured and model-free determination of all ocular surfaces, with decreased patient motion from the faster SSOCT system, and with direct measurement of the system-to-cornea distance (see SA1.Research Design.*System Calibration*). With these improvements, we anticipate that we will decrease the curvature difference between MRI and OCT to less than a millimeter (resolution of our MRI). Further, we will compare surface topographies of myopic patients with known morphometric changes (e.g. staphylomas) imaged with MRI and OCT.

SA3. Research Design. *Algorithm development and validation.* We will extend our previously developed three-dimensional refraction correction algorithms [20] to perform ray tracing of the OCT scan paths through the ocular surfaces contained within the whole eye OCT images. The anterior eye image content will be segmented and corrected of optical distortions as in Aim 2 (refraction, non-telecentricity, motion). Group refractive indices for our light source (λ_0 = 1060 nm) will be used for refraction correction as described in detail in SA2.Research Design.*Algorithm Development*. For the lens, we will measure the group index for IOLs, and use a polynomial model for natural lenses [52] as was used in our pilot work [4]. The retinal layers of the posterior eye will also be segmented in preparation for post-processing [53]. With a known system topology, measured and hence known system-to-cornea distance per patient, and an accurate representation of the anterior eye components, we will determine the spatial orientation of the OCT scan paths to the posterior eye. With these OCT scan paths, the posterior eye A-scans will be properly repositioned spatially to restore anatomic accuracy.

We will validate the algorithms by imaging a constructed model eye. The model consists of a custom-made +30 D rigid gas permeable contact lens (Essilor, center thickness 490 μm), a +20 D intraocular lens (SA60AT, Alcon), and a glass hemisphere with a 12.5 mm radius of curvature (64-496, Edmund Optics). These will be mounted into a lens tube at physiological distances and then immersed into balanced salt solution, leaving only the anterior surface of the contact lens ("cornea") exposed. The model eye will be imaged with the whole eye OCT and the surfaces recovered. After correction with the above algorithms, the curvature of the hemisphere will be compared to that of the manufacturer reference.

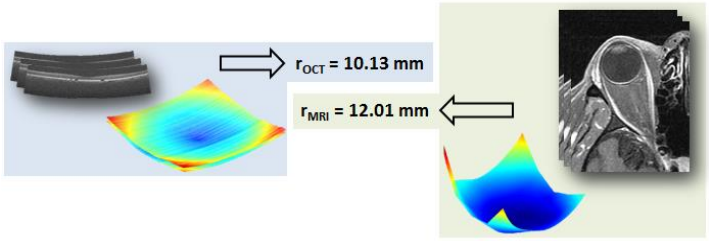

FIGURE 10. General overview of clinical study design to determine the difference between OCT and MRI posterior eye images. Using radius of curvature as a general measure of shape, we will compare the paired differences between the two modalities. In a second study in subjects with staphylomas, we will use root mean square difference to describe the topographic differences between the two registered modalities.

Clinical study. For the clinical studies, we will enroll two groups of subjects: 1. pseudophakic subjects with no known history of ocular pathology other than refractive error (no more than -6 D) and 2. pseudophakic and phakic subjects with high progressive myopia including those with staphylomas.

Group 1. The goal for the first group is to demonstrate in a normal eye the ability to accurately recreate the posterior eye with OCT spatially comparable to MRI (Fig. 10). We will only include monofocal pseudophakic individuals in this group. This reduces uncertainties by using a known manufactured lens. At the Duke Eye Center, the monofocal lens of choice is manufactured by Alcon, and the company has provided us with the optical prescriptions of their IOLs for research use under a non-disclosure agreement. With the optical properties of the IOL known, we anticipate being able to fully characterize these normal, pseudophakic eyes optically. This also provides a baseline from which phakic eyes can be studied.

Each enrolled subject will undergo the following imaging: optical biometry (LenStar, Haag-Streit), whole eye OCT, and MRI imaging. MRI will be performed on the clinical research scanners at the Duke Brain Imaging and Analysis Center (see support letter from director Dr. Allen Song). Annually, with the assistance of dedicated research coordinators, they image over 2000 subjects with MRI for over 70 research projects. Their scanner (GE) has a magnetic field strength of 3.0 Tesla. A high resolution T1 FSPGR sequence will be used to acquire images of the subject's eyes. Images will be acquired in the axial plane, with FOV=25.6cm, TR=8ms, TE=3ms, flip angle=12, 512x512x50 imaging matrix, completely covering the eyes. A second T2 weighted sequence will be acquired at the same slice prescription with TR=3s and TE=25ms. With these scan parameters, each voxel will be 0.5 mm^3. During scanning, a fixation target will be provided to minimize eye motion during acquisition.

The radius of curvature of the posterior eye will be measured via surface fitting of the posterior eye data from OCT and MRI. To have 80% power to detect a 0.5 mm difference in radius of curvature between OCT and MRI using a paired one-sample t-test, we will need to enroll a minimum of 48 normal pseudophakic subjects (PROC POWER, SAS v9.3). This power calculation assumes that with our whole eye OCT and improved algorithms, we will halve the standard deviation of the difference between MRI and OCT found in our initial study (2.3 mm), resulting in an estimated standard deviation of 1.2 mm. At a 0.5 mm difference, we will be at the effective voxel resolution of the MRI scans and should also have more than enough resolution to identify the large-scale topographic abnormalities noted in previous MRI studies of myopia [25,26].

Group 2. After enrollment and data analysis of the first group, we will then examine the ability of OCT to provide spatially comparable images to MRI in eyes that are structurally abnormal. We will enroll 20 adult patients with progressive high myopia (more than -6 D) especially targeting those with posterior staphylomas – outpouchings of the posterior eye. These subjects can be pseudophakic or phakic. Phakic subjects will be required to be cyclopleged to ensure no dynamic lens changes during imaging. For phakic reconstructions, we will use age appropriate models of the natural lens indices as we have used in our previous study [52]. After recovery of the OCT and MRI surfaces, the OCT surface will be registered to the MRI surface at a common feature (e.g. optic nerve) and via cross-correlation. A root mean square deviation across the registered surfaces will then be calculated to quantify the topographic difference between the OCT and MRI surfaces.

SA3. Expected Outcomes. At the conclusion of this aim, we will have developed algorithms to spatially correct full eye OCT images and validated them with reference phantoms. We will also have tested the idea that spatially corrected OCT images will be comparable to MRI representations of the posterior eye first in pseudophakic normal eyes and then in psuedophakic and phakic myopic eyes. This will provide the basis for OCT to replace MRI for ophthalmic studies of ocular morphometry, lowering cost and logistical barriers to these types of studies while also providing higher resolution images over MRI. This has clinical utility for study of myopia progression and risk stratification based on prior studies associating deviations in ocular shape with pathologic myopia.

SA3. Potential Problems & Alternative Strategies. The FOV of our proposed posterior eye OCT channel will be 85° (or ~120° relative to center of the eye) – at least double that of standard retinal photography. This should be sufficient for measuring posterior eye shape as it encompasses the entire macula and reaches nearly to the equator of the eye. Should larger FOV be desired, though, we can use montaging as others have shown with OCT [54] to further increase our FOV. Because our whole eye OCT also concurrently images the anterior eye, our reconstructions can account for the relative change in position between the system and the eye to increase the accuracy of montaging and provide additional references for montage reassembly.

While the natural lens does present an ambiguity, by first imaging pseudophakic subjects in group 1 and part of group 2, we will first refine and validate our algorithms independent of the natural lens. This lays the foundation for subsequently investigating and isolating any differences between MRI and OCT resulting from imaging phakic subjects in group 2. Our preliminary algorithm using a polynomial gradient index lens model [52] demonstrated reduced differences between OCT and MRI [4]. Alternate OCT based natural lens models [55] can be incorporated into our reconstructions for reanalysis of captured and stored image data if necessary. Our use of these gradient indices is far more sophisticated than the average refractive indices successfully used for ocular axial biometry both in research and clinically [56,57 and commercially available partial coherence interferometers]. If necessary, we can similarly use average indices. Importantly, with the validated pseudophakic group, we will be able to compare and contrast quantitative performance of OCT in phakic subjects. This data has important implications for both the OCT and myopia communities.

Timetable. We anticipate this ambitious project will require the full requested five year project period to complete. We anticipate the whole eye SSOCT system design and assembly will take approximately one year. Algorithm development will begin with initial images of phantoms and normals and can occur concurrently with clinical imaging because all acquired images can be post-processed at a later date if necessary. Data collection, data analysis, and publication will occur on a rolling basis throughout the project.